Open access • Journal Article • DOI:10.1108/03321640810861098

Probabilistic methods applied to 2D electromagnetic numerical dosimetry
— Source link ↗

Damien Voyer, François Musy, Laurent Nicolas, Ronan Perrussel

Institutions: École centrale de Lyon

Topics: Probabilistic logic, Monte Carlo method, Polynomial chaos, Sparse grid and Probabilistic method

Related papers:

- Variability on the Propagation of a Plane Wave Using Stochastic Collocation Methods in a Bio Electromagnetic Application

- Combined Approximations for Efficient Probalistic Analysis of Structures

- High Dimensional Stochastic Simulation and Electric Ship Models

- Finite-element/progressive-lattice-sampling response surface methodology and application to benchmark probability quantification problems

- Probabilistic load flow computation using saddle-point approximation

Probabilistic methods applied to 2D electromagnetic numerical dosimetry

Damien Voyer, François Musy, Laurent Nicolas, Ronan Perrussel

Probabilistic methods applied to 2D electromagnetic numerical dosimetry

D. Voyer[*]   F. Musy[†]   L. Nicolas[*]   R. Perrussel[*]

Abstract

Purpose   Probabilistic approaches are performed on electromagnetic numerical dosimetry problems in order to take into account the variability of the input parameters.

Methodology/Approach   Methods are based on an expansion of the random parameters in two different ways: a spectral description and a nodal description.

Findings   It is shown on a simple scattering problem that only 100 calculations are required applying these methods while the Monte Carlo method uses 10 000 samples for a comparable accuracy.

Originality/value of paper   The number of calculations is dramatically reduced using different techniques: a regression technique, sparse grids computed from Smolyak's algorithm or a suited coordinate system.

Keywords   Numerical dosimetry, electromagnetism, stochastic method, polynomial chaos, sparse grid.

Paper type   Research paper.

[*]Laboratoire Ampère; CNRS, UMR 5005; Ecole Centrale de Lyon, 69134 Ecully FRANCE.
[†]Institut Camille Jordan; CNRS, UMR 5208; Ecole Centrale de Lyon.

1 Introduction

Electromagnetic dosimetry attempts to evaluate the interaction between electromagnetic waves and biological tissues; the coupling between the electromagnetic field radiated by a cellphone and the human body is an illustrative example. Numerical simulations are the only tool to estimate accurately the specific absorption rate – SAR – in the human body [Leveque et al., 2004, Scorretti et al., 2004]. Up to now most of the works has been focused on determinist problems in which the values of the input parameters are supposed to be certain. However, these parameters are inherently known with some vagueness; uncertainties appear indeed in the description of the human body – *e.g.* the nature of tissues or the morphology – but also in the description of the source – *e.g.* the position of the cellphone or the frequency – [Stavroulakis, 2003, Hurt et al., 2000]. Thus, determinist calculations are not suited to properly describe the complexity of the problem. This issue is particularly crucial in the normative context.

In order to obtain statistic information such as the mean or the variance of the SAR, the Monte Carlo method could be applied [Newman et al., 1999]. However, the convergence rate of the method is slow: $1/\sqrt{K}$ where K denotes the number of realizations. When the modeling of the 3D interaction between the human body and a cellphone is considered with many details in the morphology, one calculation already requires large computational resources. This consequently makes prohibitive the use of the Monte Carlo method. To deal with this issue, another method – the spectral stochastic finite element method – has been introduced in mechanics in the early nineties [Ghanem and Spanos, 1991]. It is based on a spectral decomposition of the random space using the polynomial chaos. There are two approaches: the so called intrusive method where the determinist solution is widely recast [Ghanem and Kruger, 1996] and the so called non intrusive method that uses determinist computations with a restrictive number of realizations *a priori* chosen [Ghiocel and Ghanem, 2002]. In

this paper, we will focus our attention on the non intrusive method because of the limitation of the numerical resources. Indeed, the intrusive method leads to an algebraic system that is larger than the system built in the determinist case. This is a serious drawback in complex problems where these matrix systems are already large in the determinist case. Completing the previous strategy, a collocation method using Lagrange polynomial has recently came out [Chauvière et al., 2006]. This technique is an alternative method to reduce the number of realizations; the difference with spectral methods lies on the fact that the description of the random variable is based on a nodal approach. The numerical cost can be further decreased using a regression approach, sparse grids computed from Smolyak algorithm or a suited coordinate system.

In electromagnetism, only few works have been led; let's however quoting two significant examples: the intrusive spectral stochastic finite element method has been applied to an electrostatic problem where the permittivity of materials is described by a random law [Gaignaire et al., 2007]; the collocation method has been implemented in a scattering problem where uncertainty is introduced in the source term, in the geometrical shape and in the material [Chauvière et al., 2006]. The objective of this paper is to show the feasibility of the probabilistic methods in electromagnetic dosimetry. For this purpose, non intrusive methods are used and several developments, such as the sparse grid or the suited coordinate system, are investigated to reduce the numerical costs. In order to evaluate their accuracy, the electromagnetic problem has been reduced to a 2D problem so that the results can be compared with those obtained by the Monte Carlo method.

2 Some probability concepts

2.1 Expansion of random variables

2.1.1 Related Hilbert space

The manipulated random variables are supposed to be described in the vector space of random variables with finite variance that is denoted $L^2(\Omega, P)$, where Ω is the sample space and P a probability measure on Ω.

A continuous random variable X of this space is characterized by a probability density function f_X. The mathematical expectation $E[X]$ is then given by:

$$E[X] = \int_{-\infty}^{+\infty} x f_X(x) \, dx. \tag{1}$$

It can be shown that the space $L^2(\Omega, P)$ is a Hilbert space with the inner product and the norm defined as follow:

$$\langle X, Y \rangle = E[XY] \text{ and } \|X\| = \sqrt{E[X^2]}. \tag{2}$$

Any random variable of $L^2(\Omega, P)$ can be expanded on the polynomial chaos – this is the spectral description – or be interpolated using Lagrange polynomials – this is the nodal description –.

2.1.2 Spectral description

Let us suppose that X is a random variable depending on a single random parameter. It can be expressed from a canonical random variable such as a normal or a uniform random variable [Schoutens, 2000]. Let us take for example a standard normal variable ξ. Then X can be decomposed as follow:

$$X = \sum_{j=0}^{+\infty} X_j H_j(\xi), \tag{3}$$

where $\{H_j\}_{j=1}^{+\infty}$ denotes the sequence of Hermite polynomials. In particular one has $H_0 = 1$, $H_1 = \xi$ and $H_2 = \xi^2 - 1$. The Hermite polynomials form an

orthogonal basis with respect to the inner product defined in (2):

$$E\left[H_i H_j\right] = i!\,\delta_{ij}, \ \forall i,j \in \mathbb{N}, \tag{4}$$

where δ_{ij} is equal to one if $i = j$ and else is equal to zero.

Let us now suppose that X is a random variable depending on D random parameters. Then X can be expressed introducing as many standard normal variables $\xi_1, \xi_2, ..., \xi_D$ as there are random parameters:

$$X = \sum_{j=0}^{+\infty} X_j \psi_j\left(\xi_1, \xi_2, \ldots, \xi_D\right), \tag{5}$$

where $\{\psi_j\}_{j=1}^{+\infty}$ denotes the polynomial chaos. Those polynomials are built from a product of unidimensional Hermite polynomials:

$$\psi_j\left(\xi_1, \xi_2, \ldots, \xi_D\right) = \prod_{i=1}^{D} H_{\alpha_i}\left(\xi_i\right), \tag{6}$$

where $\sum_{i=1}^{D} \alpha_i = d_j$ with d_j the total degree of the polynomial ψ_j.

In the numerical implementation, the total degree of the polynomial chaos is limited to a value d. The dimension of the polynomial space is then $\binom{D+d}{d}$ and it grows fast with D or d.

2.1.3   Nodal description

In the univariate case, X can be interpolated from P collocation points $\{\xi^p\}_{p=0}^{P-1}$ using Lagrange polynomials:

$$X_{\text{interp}} = \sum_{j=0}^{P-1} \widetilde{X}_j L_j\left(\xi\right), \tag{7}$$

where Lagrange's polynomials L_j are defined by:

$$L_j(\xi) = \prod_{\substack{p=0 \\ p \neq j}}^{P-1} \frac{\xi - \xi^p}{\xi^j - \xi^p}, \tag{8}$$

in order to satisfy:

$$L_j(\xi^i) = \delta_{ij}, \ \forall i, j \in [\![0; P-1]\!]. \tag{9}$$

In the multivariate case, X can be interpolated from a product of unidimensional Lagrange polynomials.

2.2 Statistic information from determinist codes

Let us consider X the output random variable of the problem. For a better understanding, only the case of a single input random variable will be treated; the random space can then be described by a single normal variable ξ. The problem is to approximate the random variable X using the same code as for determinist computations. The methods presented here evaluate the approximate solution from few realizations of the input random variable ξ *a priori* determined.

2.2.1 Projection method

In the numerical implementation, the expansion given in (3) is truncated to an order $P - 1$ so that the approximate solution is expressed as:

$$X_{\text{appr}} = \sum_{j=0}^{P-1} X_j H_j(\xi). \tag{10}$$

The projection method is based on the orthogonality property of the Hermite polynomials [Puig et al., 2002]. From (3), one finds:

$$X_j = \frac{E[X H_j]}{E[H_j^2]}, \ \forall j \in [0, P-1]. \tag{11}$$

In (11), the difficulty is to evaluate the numerator:

$$E\left[X H_j\right] = \int_{-\infty}^{+\infty} X\left(\xi\right) H_j\left(\xi\right) \frac{e^{-\frac{\xi^2}{2}}}{\sqrt{2\pi}}\, d\xi. \tag{12}$$

The integral in (12) can be approximated by using the gaussian quadrature formula:

$$E\left[X H_j\right] \approx \sum_{p=0}^{P-1} w_p\, X\left(\xi^p\right) H_j\left(\xi^p\right)$$
$$\text{with } w_p = \frac{(P-1)!}{H_P'\left(\xi^p\right) H_{P-1}\left(\xi^p\right)}, \tag{13}$$

where $\{\xi^p\}_{p=0}^{P-1}$ are the roots of the Hermite polynomials of order P.

From the truncated expansion (10), the whole probabilistic information of X can be approximated. For example, the mean μ and the variance σ^2 are given by:

$$\mu = E\left[X\right] = X_0,$$
$$\sigma^2 = E\left[(X-\mu)^2\right] \approx E\left[(X_{\text{appr}} - \mu)^2\right] = \sum_{j=1}^{P-1} X_j^2\, j!\,. \tag{14}$$

2.2.2 Least square minimization

The method is based on a least square minimization of the discrepancy between the input variable X and its truncated approximation X_{appr} given in (10) [Webster et al., 1996]. The technique consists in minimizing the error between X and X_{appr} at K points $\{\xi^k\}_{k=1}^{K}$ expressed by:

$$\text{err} = \sum_{k=1}^{K} \left(X\left(\xi^k\right) - X_{\text{appr}}\left(\xi^k\right)\right)^2. \tag{15}$$

Minimizing err leads to the following linear system:

$$\sum_{k=1}^{K} \begin{bmatrix} H_0 H_0 & \cdots & H_0 H_{P-1} \\ \vdots & \ddots & \vdots \\ H_0 H_{P-1} & \cdots & H_{P-1} H_{P-1} \end{bmatrix}_{\xi=\xi^k} \begin{bmatrix} X_0 \\ \vdots \\ X_{P-1} \end{bmatrix} = \sum_{k=1}^{K} \begin{bmatrix} X H_0 \\ \vdots \\ X H_{P-1} \end{bmatrix}_{\xi=\xi^k}. \tag{16}$$

Usually the points $\left\{\xi^k\right\}_{k=1}^K$ are chosen to be the roots of an Hermite polynomial of degree equal or higher than P.

2.2.3   Collocation method

The collocation method is based on a nodal description [Chauvière et al., 2006]. From (7), it is required that the residual $X\left(\xi\right) - X_{\text{interp}}\left(\xi\right)$ is zero at the collocation points $\left\{\xi^p\right\}_{p=0}^{P-1}$. The property reported in (9) immediately gives the value of $\widetilde{X}_j$:

$$\widetilde{X}_j = X\left(\xi^j\right). \tag{17}$$

It seems natural to choose the collocation points $\left\{\xi^p\right\}_{p=0}^{P-1}$ as the roots of the Hermite polynomial of order P since ξ is a normal variable.

As for the spectral description, the whole probabilist quantities can be extracted from the nodal approach. For example, the mean μ is given by:

$$\mu \approx E\left[X_{\text{interp}}\right] = \sum_{j=0}^{P-1} \widetilde{X}_j \int_{-\infty}^{+\infty} L_j\left(\xi\right) \frac{e^{-\frac{\xi^2}{2}}}{\sqrt{2\pi}}\, d\xi. \tag{18}$$

The integral can be evaluated using the gaussian quadrature formula. One finds:

$$\mu \approx \sum_{j=0}^{P-1} w_j \widetilde{X}_j \tag{19}$$

where w_j are the weights associated to the roots of the Hermite polynomial of degree P given in (13).

2.3   Reduction of the number of calculations

When a lot of random variables are required for the problem, the methods described in the previous section become less efficient since more determinist calculations have to be performed. In order to reduce the numerical cost, several techniques can be applied.

8

2.3.1   Sparse grids

Sparse grids can be used to choose a restrictive number of nodes either with the projection method or with the collocation method. Let us consider first the case of the projection method. In the multivariate case, (12) involves the polynomial chaos defined in (5) and becomes:

$$E\left[X\,\psi_j\right] = \int_{\mathbb{R}^D} \left(X\psi_j\right)(\xi_1,\cdots,\xi_D)\,\frac{e^{-(\xi_1^2+\cdots+\xi_D^2)/2}}{(2\pi)^{D/2}}\,d\xi_1\ldots d\xi_D. \qquad (20)$$

In order to evaluate (20), univariate quadrature rules can be extended to multiple dimensions by an appropriate tensor product rule:

$$E\left[X\,\psi_j\right] \approx \sum_{\xi_1\in\mathbb{P}_{p_1}} \cdots \sum_{\xi_D\in\mathbb{P}_{p_D}} \left(X\psi_j\right)(\xi_1,\ldots,\xi_D) \prod_{m=1}^{D} w_{p_m}(\xi_m)$$
$$= \left(V_{p_1}\otimes\ldots\otimes V_{p_D}\right)\left(X\psi_j\right) \qquad (21)$$

where the set of nodes $\{\mathbb{P}_{p_1},\ldots,\mathbb{P}_{p_D}\}$ and weights $\{w_{p_1},\ldots,w_{p_D}\}$ are those implied by the underlying unidimensional quadrature rules $\{V_{p_1},\ldots,V_{p_D}\}$. Consequently, the product rule evaluates the function $X\psi_j$ at the full grid of points $\mathbb{P}_{p_1}\otimes\ldots\otimes\mathbb{P}_{p_D}$. In D dimensions, the product rule therefore requires P^D evaluations of the function $X\psi_j$ if the underlying univariate rules are all based on P nodes. While for example a gaussian quadrature rule exactly evaluates a univariate polynomial of order 7 with 4 function evaluations, the corresponding product rule with 10 dimensions requires $4^{10} = 1\,048\,576$ evaluations which is generally prohibitive.

Smolyak proposed an algorithm to evaluate integrals over several dimensions with a substantially smaller number of function evaluations than the product rule [Xiu and Hesthaven, 2005]. This is achieved by combining sequences of univariate rules with different accuracy levels. The set of nodes used by the

sparse grids rule can be written as:

$$\mathbb{P}_{D,k} = \bigcup_{q=k-D}^{k-1} \bigcup_{\mathbf{p} \in \mathbb{N}_q^D} \mathbb{P}_{p_1} \otimes \ldots \otimes \mathbb{P}_{p_D} \tag{22}$$

where $\mathbf{p} = \{p_1, \ldots, p_D\}$ and:

$$\mathbb{N}_q^D = \left\{ \mathbf{p} \in \mathbb{N}^D : \sum_{i=1}^{D} p_i = D + q \right\} \tag{23}$$

when $q \geq 0$ and $\mathbb{N}_q^D = \emptyset$ when $q < 0$; for instance $\mathbb{N}_2^2 = \{[2,2], [1,3], [3,1]\}$.

Figure 1 shows the construction of the sparse grid by the Smolyak rule in a simple example with $D = 2$ and $k = 3$. The nodes for a sequence of univariate quadrature rules $\mathbb{P}_1$, $\mathbb{P}_2$ and $\mathbb{P}_3$ are shown in the top of the figure. The product rule $\mathbb{P}_3 \otimes \mathbb{P}_3$ evaluates the function at all two-dimensional combinations of nodes prescribed by $\mathbb{P}_3$ which are shown in the upper right part of the figure. As expressed in (22), the sparse grids rule combines tensor products of lower degree $\mathbb{P}_i \otimes \mathbb{P}_j$ such that $3 \leq i + j \leq 4$. The nodes of these products as well as the resulting sparse grid are shown in the lower part of the figure. The integral over multiple dimensions given in (20) can then be approximated by:

$$E[X\psi_j] \approx \sum_{q=k-D}^{k-1} (-1)^{k-1-q} \binom{D-1}{k-1-q} \sum_{\mathbf{p} \in \mathbb{N}_q^D} (V_{p_1} \otimes \ldots \otimes V_{p_D})(X\psi_j). \tag{24}$$

Sparse grids can also be exploited with the collocation method: the selected nodes given in (22) are used to build a Lagrange polynomial basis.

2.3.2 Regression method

This technique is derived from the least square minimization. In (16), it appears that the linear system is built in a cumulative way: at each new iteration k, terms depending on ξ_k are added to the matrix and to the second member which had been obtained in the previous iteration $k - 1$. Consequently, it is possible to solve this matrix equation without performing the whole of the K
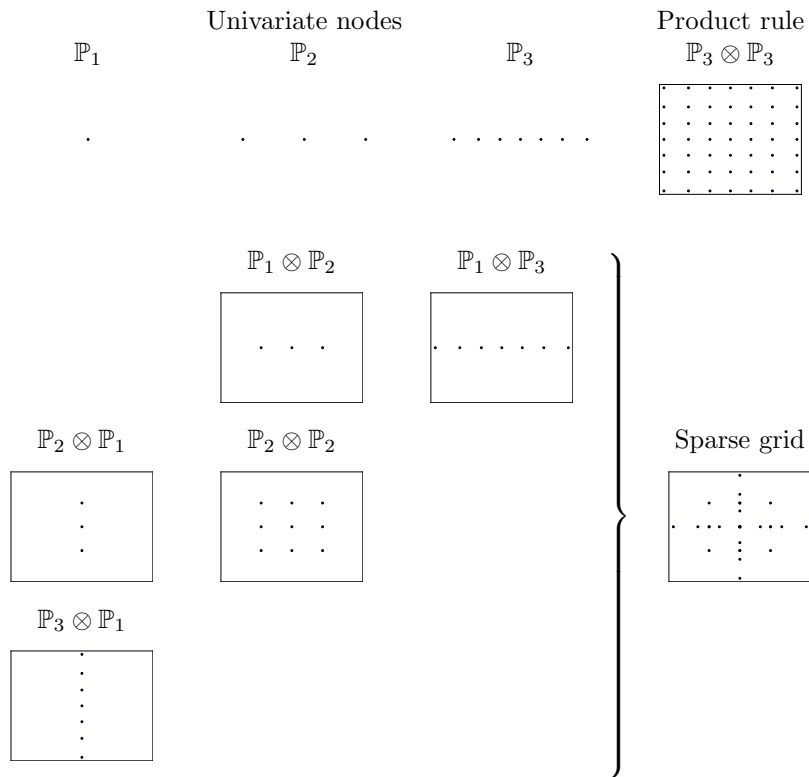
Figure 1: an example of sparse grid.

computations. This is the aim of the regression method: the solution is calcu-
lated for each iteration k and the algorithm is stopped when the convergence is
achieved [Berveiller et al., 2006]. The points $\left\{\xi^k\right\}_{k=1}^K$ are organized according
to the greatest density probability.

2.3.3 Choice of the coordinate system in the random space

The efficiency of probabilistic approaches depends actually on a judicious choice
of the coordinate system in the random space. The expansion of random varia-
bles using the Hermite polynomials was at the very beginning a spectral repre-
sentation of the fields built from normal variables [Wiener, 1938]. However, the
convergence turns out to be slow when the random variables are not normal.
Let us consider for example a random variable X characterized by a uniform law

on the interval $[X_a, X_b]$. The representation using a standard normal variable ξ_G can be calculated analytically [Field and Grigoriu, 2004]:

$$X = \frac{X_a + X_b}{2} H_0\left(\xi_G\right) + \sum_{j=0}^{+\infty} \frac{(-1)^j \eta_j}{\sqrt{\pi} \, 2^j \, (2j+1)!} \frac{X_b - X_a}{2} H_{2j+1}\left(\xi_G\right), \qquad (25)$$

where $\eta_j = |-1 \times 1 \times 3 \times \ldots \times (2j-1)|$.

However, using a uniform variable ξ_U defined in the interval $[-1, 1]$, the expansion on the Legendre polynomials is immediately given by:

$$X = \frac{X_a + X_b}{2} Lg_0\left(\xi_U\right) + \frac{X_b - X_a}{2} Lg_1\left(\xi_U\right) \qquad (26)$$

where $\{Lg_j\}_{j=0}^{+\infty}$ is the sequence of Legendre polynomials. In particular, one has $Lg_0 = 1$ and $Lg_1 = \xi_U$. The Legendre polynomials form an orthogonal basis with respect to the inner product defined in (2).

Thus a suited choice of the coordinate system improves the convergence in the representation of the random variables and consequently leads to a better accuracy of the probabilistic methods. This approach has recently been developed through the generalized polynomial chaos: the polynomial basis is built according to the nature of the distribution of random variables [Xiu and Karniadakis, 2002].

3   Application in electromagnetic dosimetry

3.1   Description of the problem

Electromagnetic dosimetry deals with the problem of the interaction between the human body and the electromagnetic field in the low frequency range or the high frequency range. The methodology described here may be applied in low frequency problem but this is not considered in the present paper. In high frequency, the problem concerns the coupling between the human body and the electromagnetic waves radiated from a cellphone or an antenna. This issue may become very complex if a realistic scene is modeled. In this paper, the

problem is reduced to a 2D geometry so that the Monte Carlo method can be applied for comparison. The geometry of the problem is described in Figure 2; it could be the leg of a human adult that is modeled by an infinite cylinder with different layers to take into account the presence of different biological tissues; three layers characterized by different permittivities and conductivities are introduced to describe bone, muscle and fat. The structure is illuminated by an incident plane wave or by an infinitely long filament source in free space. Thus the electromagnetic problem is invariant following the direction of the cylinder axis and a symmetry appears.
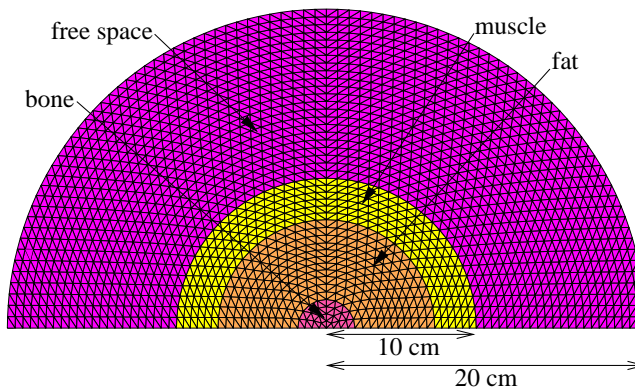

Figure 2: the 2D geometry problem.

To solve numerically this problem, the finite element method has been implemented with second order absorbing boundary conditions allowing the scattering waves to radiate out of the domain [Bayliss and Turkel, 1980]. The frequency is set about to 1.2 GHz and 3 000 to 4 000 elements are used for the discretization. The effects of the electromagnetic waves in the body are quantified by calculating the SAR ; it measures the quantity of electromagnetic power absorbed by 1 kg of tissue:

$$SAR = \frac{1}{2}\frac{\sigma E^2}{\rho} \; (\text{W/kg}) \tag{27}$$

where σ is the conductivity of the tissue, ρ is the mass density of the tissue and E the amplitude of the electric field. In this paper, we are interested in the maximal SAR locally absorbed in the body.

13

In order to properly describe the reality, the variability that appears in the properties of the tissues – permittivity and conductivity – but also in the morphology – thickness of the tissues – or in the characteristics of the source – frequency and position of the punctual source – has to be introduced. The problem consists then in evaluating how those uncertainties affect the maximal SAR in the leg.

3.2 Statistic calculations using the Monte Carlo method

To calculate the statistic response of the maximal SAR, the Monte Carlo method can be applied. Using a given number of samples, one calculates the maximal value of SAR for each realization. The estimated mean μ_{SAR} and variance σ^2_{SAR} can then be computed as follows:

$$\mu_{SAR} = \frac{1}{K} \sum_{k=1}^{K} SAR_k \quad \text{and} \quad \sigma^2_{SAR} = \frac{1}{K} \sum_{k=1}^{K} (SAR_k - \mu_{SAR})^2, \qquad (28)$$

where K is the total number of samples and $\{SAR_k\}_{k=1}^{K}$ are the values of the maximal SAR for the K realizations.

In the first example treated in this paper, an incident transverse electric wave whose electric field has an amplitude $E = 1 \text{ Vm}^{-1}$ illuminates the leg. Some randomness is introduced in the properties of the tissues. More precisely, the permittivity and the conductivity of the three kinds of tissues are considered to be random variables with lognormal distributions. The mean values of these parameters are obtained from [Council,] – see also [C.Gabriel and E.Corthout, 1996] –. The variance values have been chosen arbitrarily in order to compare the robustness of the different methods. The parameters are reported in Table 1.

Figure 3 shows an illustration of the electric field and SAR computed using the mean values given in Table 1.

The repartition of the maximal SAR computed from 10 000 samples is given in Figure 4. The mean and the variance estimated from those data are equal to $\mu_{SAR} = 5.19\,10^{-5} \text{ Wkg}^{-1}$ and $\sigma^2_{SAR} = 1.31\,10^{-10} \text{ W}^2\text{kg}^{-2}$.

Quantity	Mean	Variance
Relative permittivity of bone	12.2	0.6
Conductivity of bone (Sm^{-1})	0.185	0.030
Relative permittivity of muscle	54.4	1.0
Conductivity of muscle (Sm^{-1})	1.055	0.100
Relative permittivity of fat	5.41	0.04
Conductivity of fat (Sm^{-1})	0.0580	0.0008

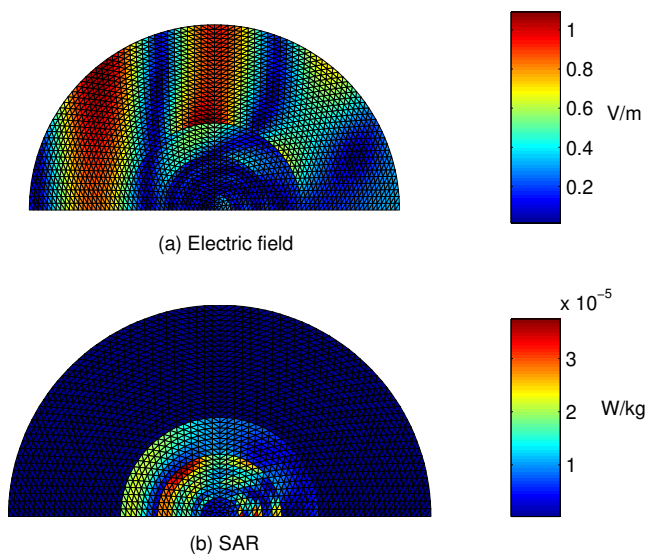Table 1: parameters of the different lognormal laws.

(a) Electric field

(b) SAR

Figure 3: electric field and SAR computed for the first example with the mean values of the parameters given in Table 1.

3.3 Probabilistic calculations using a spectral description

The space of random variables is built from the polynomial chaos made of six normal variables to describe the six uncertain tissue parameters. The total degree of the polynomials is first limited to $d = 2$; this leads to consider 28 polynomials. The total degree d is too low to accurately describe the lognormal laws but it already implies $3^6 = 729$ determinist calculations if spectral methods are applied as they are initially proposed. The results concerning the mean are close to those obtained with the Monte Carlo method – the relative difference is
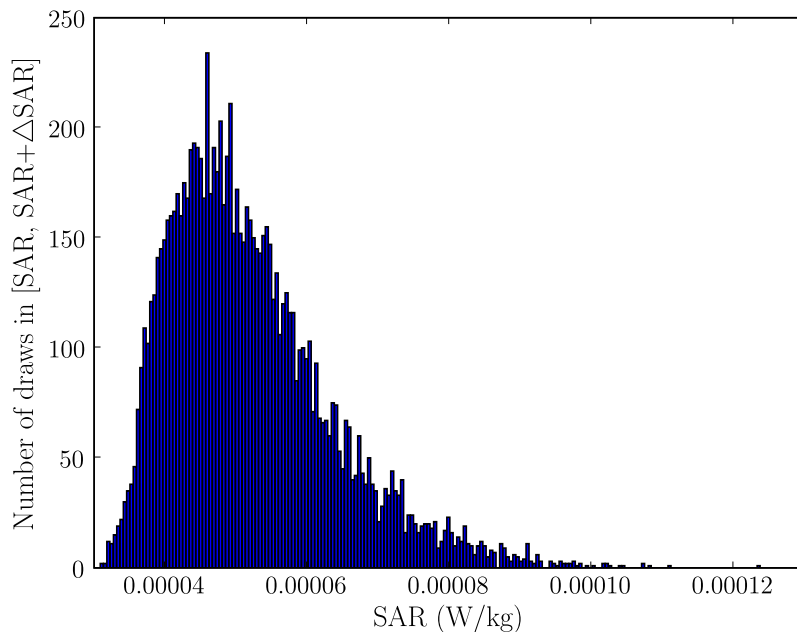
15

Figure 4: repartition of the maximal SAR calculated from 10 000 samples.

less than 1% – but there is a difference concerning the variance: roughly 17% for the projection method and 12% for the least square method – see Table 2 –. In order to refine the result, the total degree d is increased to 4; 210 polynomials are then handled. However, there would be *a priori* $5^6 = 15\,625$ determinist calculations to make, which goes beyond the number of calculations realized using the Monte Carlo method.

To reduce this number using the projection method, sparse grids have been experimented. The nodes for the sequence of univariate quadrature rules $\mathbb{P}_1$, $\mathbb{P}_2$ and $\mathbb{P}_3$ are set to be the roots of Hermite polynomials of degree 1, 3 and 5. This choice is such that zero is a root shared by the three sequences; consequently, the construction of the Smolyak grid leads to a lower number of nodes. In this case, the sparse grid $\mathbb{P}_{6,3}$ is composed of 97 nodes instead of $15\,625$ nodes for the product rule. But the variance calculated using this grid is far from the expected value; this is due to the fact that Smolyak algorithm guaranties

a small error when the degree of the integrand $X\psi$ in (20) is not too large [Xiu and Hesthaven, 2005]. In the present case, the degree of X is *a priori* infinite; however, the weight of higher degree components decreases more and less fast following the non linear dependence on the input random variables. To take into account higher degree components in integral computations, the sparse grid has to be extended. For example, a fourth sequence $\mathbb{P}_4$ composed with the roots of the Hermite polynomial of degree 7 can be added. The sparse grid $\mathbb{P}_{6,4}$ then counts 533 nodes. The computed results are more accurate; the variance is closer to the one calculated with the Monte Carlo method – the relative difference is roughly 8%; see Table 2 –.

To save numerical cost using the least square approach, the regression method can be applied by increasing progressively the numbers of nodes. The analysis reported on Figure 5 shows that the value of the variance converges when K is close to 800 and the result is not so far from the one evaluated using the Monte Carlo method – the relative difference is approximately 2%; see Table 2 –.
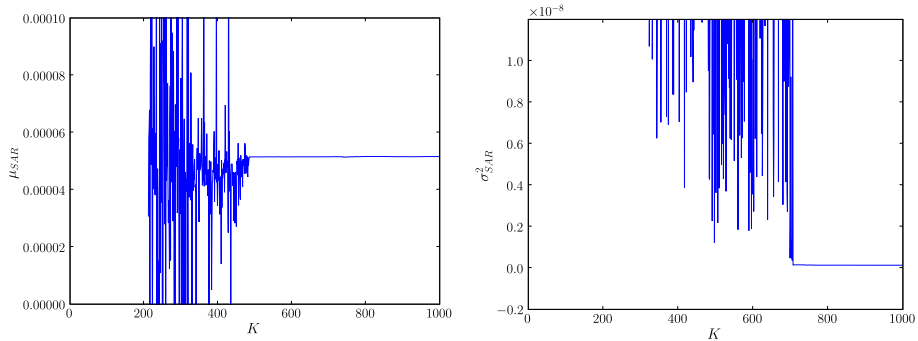
(a) estimated mean μ_{SAR} against the number of nodes K.

(b) estimated variance σ^2_{SAR} agings the number of nodes K.

Figure 5: study of convergence using the regression method.

3.4 Probabilistic calculations using a nodal description

A Lagrangian basis is first built from the product rule using the roots of the Hermite polynomial of degree 3; that is to say the basis is composed of $3^6 = 729$

Method	Number of realizations	μ_{SAR} in Wkg^{-1}	error on μ_{SAR}	σ^2_{SAR} in W^2kg^{-2}	error on σ^2_{SAR}
Monte Carlo	10 000	$5.19\,10^{-5}$	-	$1.31\,10^{-10}$	-
Projection $d=2$	729	$5.17\,10^{-5}$	0.4%	$1.08\,10^{-10}$	17%
Projection $d=4$	15625	no	no	no	no
Projection $d=4$ & Smolyak $\mathbb{P}_{6,4}$	533	$5.12\,10^{-5}$	1.3%	$1.42\,10^{-10}$	8%
Least square $d=2$	729	$5.24\,10^{-5}$	0.9%	$1.15\,10^{-10}$	12%
Regression $d=4$	800	$5.16\,10^{-5}$	0.5%	$1.34\,10^{-10}$	2%

Table 2: summary of the results for the first example using spectral methods. "no" means that no computation has been performed.

polynomials. In this case, the difference of the calculated variance compared to the Monte Carlo method is lower than the one obtained with spectral methods – the relative difference is roughly 4%; see Table 3 –. A sparse grid can be built to improve this result without growing the computer resource consumption; Smolyak algorithm can be implemented using other sequences than those described in Subsection 3.3. For example, the nodes for the sequence of univariate quadrature rules $\mathbb{P}_1$, $\mathbb{P}_2$ and $\mathbb{P}_3$ can be chosen to be the roots of Hermite polynomials of degree 1, 3 and 9. Then the sparse grid $\mathbb{P}_{6,3}$ is composed of 121 nodes. The variance calculated using this grid is closer to the value obtained with the Monte Carlo method – the relative difference is approximately 1%; see Table 3 –.

Method	Number of realizations	μ_{SAR} in Wkg^{-1}	error on μ_{SAR}	σ^2_{SAR} in W^2kg^{-2}	error on σ^2_{SAR}
Monte Carlo	10 000	$5.19\,10^{-5}$	-	$1.31\,10^{-10}$	-
Collocation & roots from degree 3	729	$5.17\,10^{-5}$	0.4%	$1.25\,10^{-10}$	4%
Collocation & Smolyak $\mathbb{P}_{6,3}$	121	$5.14\,10^{-5}$	0.9%	$1.32\,10^{-10}$	1%

Table 3: summary of the results for the first example using nodal methods.

3.5 Other kind of distributions

In the second example, the source is an infinitely long filament of constant current $I = 1$ A ; this implies that the electromagnetic problem is described in the transverse magnetic mode. The position and the frequency of the source as well as the dimensions of the three tissues are supposed to be random variables with uniform distributions. The different parameters are reported in Table 4. The mean values of the morphology parameters are realistic whereas the variance values have been chosen in order to emphasize the discrepancy in the results computed by the different methods.

Quantity	Mean	Variation around the mean
Frequency (GHz)	1.2	±0.2
Position of the source (mm)	150	±10
Radius for the layer of bone (mm)	18	±5.5
Radius for the layer of muscle (mm)	59	±6
Radius for the layer of fat (mm)	94	±12

Table 4: parameters of the different uniform laws.

Figure 6 shows an illustration of the electric field and SAR computed using mean values given in Table 4.

The statistic response of the maximal SAR has been calculated using Monte Carlo method from 10 000 samples. The estimated mean and the variance are $\mu_{SAR} = 88.52$ Wkg^{-1} and $\sigma^2_{SAR} = 255.65$ W^{2}kg^{-2}. As for probabilistic methods, polynomial basis have been built in two different ways using either normal variables or uniform variables. Let us first consider the coordinate system composed by standard normal variables. The collocation method is applied. A Lagrangian basis is built from the product rule using the roots of the Hermite polynomial of degree 3; that is to say the basis is composed using $3^5 = 243$ nodes. The results are not accurate: the difference with the Monte Carlo method is roughly 1% on the mean and 7% on the variance – see Table 5 –. Let us now consider the coordinate system composed with uniform variables defined in the interval $[-1, 1]$. A Lagrangian basis is built from the product rule using the
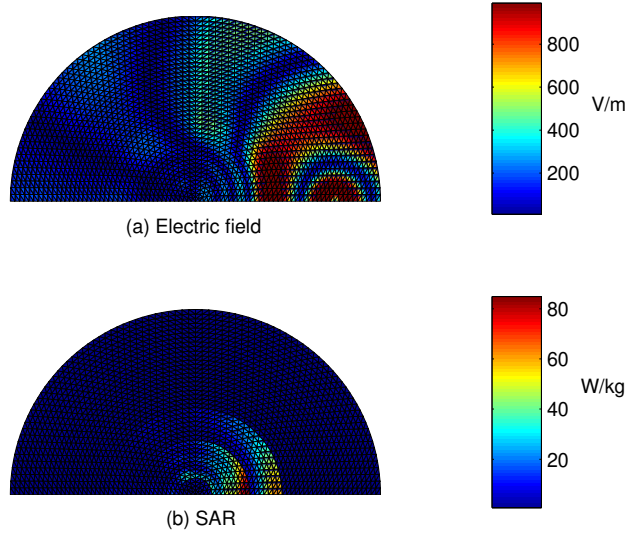
(a) Electric field

(b) SAR

Figure 6: electric field and SAR computed for the second example with the mean values of the parameters given in Table 4.

roots of the Legendre polynomial of degree 2; that is to say the basis is composed using $2^5 = 32$ nodes. Even if there are less nodes, the results are closer to the ones obtained by the Monte Carlo method: the relative difference is less than 1% on the mean and approximately 2% on the variance – see Table 5 –.

Method	Number of realizations	μ_{SAR} in Wkg^{-1}	error on μ_{SAR}	σ^2_{SAR} in W^{2}kg^{-2}	error on σ^2_{SAR}
Monte Carlo	10 000	88.5	-	255.7	-
Collocation & Hermite & roots from degree 3	243	87.6	1.0%	236.7	7%
Collocation & Legendre & roots from degree 2	32	89.1	0.7%	261.9	2%

Table 5: summary of the results for the second example.

Probabilistic methods enable to compute not only the mean and the variance but also higher order moments or the probability density function. Figure 7 shows a comparison of the probability density function of maximal SAR estimated from Monte Carlo and collocation methods. The curve obtained with

20

the collocation methods is smoother than the curve given by the Monte Carlo method. The reason is that, when using the Monte Carlo method, the probability density function is determined only from 10 000 samples which is not enough to properly describe the probability density function. On the contrary, when using collocation method, the probability density function is plotted from the nodal expansion (7) ; a larger number of points can be calculated without spending a lot of time.
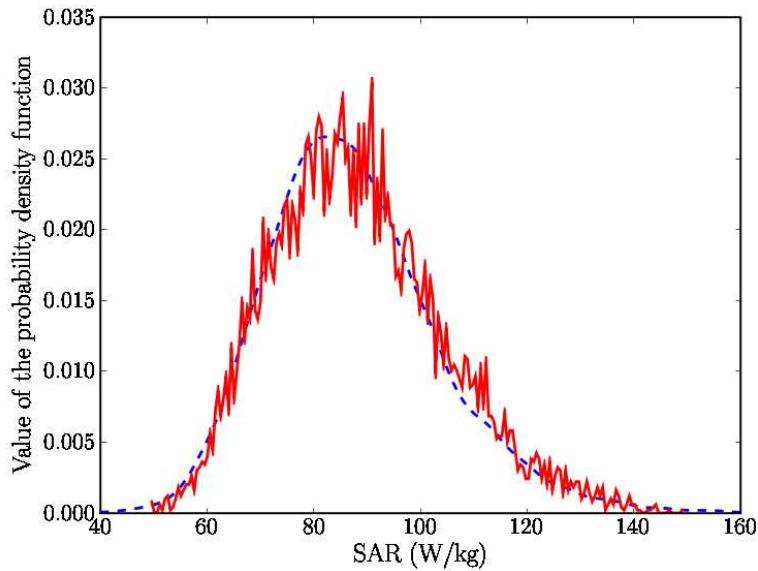

Figure 7: probability density function computed from collocation method – dashed curve – and Monte Carlo method – continuous curve –.

4   Conclusion

In this paper, the feasibility in using probabilistic methods to evaluate the stochastic response in a 2D electromagnetic dosimetry problem is demonstrated. The different approaches experimented – projection, least square minimization and collocation method – give accurate results with only a few hundreds of calculations while the Monte Carlo method involves 10 000 samples. However, the

collocation method using sparse grid seems to be the most efficient method; but one has to be wise: the accuracy depends on the specificities of the problem treated, mainly the number of random input parameters and the non linear dependence on the random input variables. To ensure the validity of the computed results, the only solution is to make a convergence study by increasing the number of nodes with the collocation method or the number of polynomials with the spectral method. The reduction of the numerical cost is essential in the perspective of studying 3D realistic situations. This issue will be the next step of this work. The difficulties to overcome concern not only numerical aspects – saving time consumption is obviously more crucial in a 3D problem than in the 2D case – but also the modelling of the variability in the human body – the choice of realistic laws for random variables or the description of the uncertainty in the morphology remain open problems –.

References

[Bayliss and Turkel, 1980] Bayliss, A. and Turkel, E. (1980). Radiation boundary conditions for wave-like equations. *Comm. Pure Appl. Math.*, 33(6):707–725.

[Berveiller et al., 2006] Berveiller, M., Sudret, B., and Lemaire, M. (2006). Stochastic finite element: a non intrusive approach by regression. *Revue européenne de mécanique numérique*, 16:81–92.

[C.Gabriel and E.Corthout, 1996] C.Gabriel, S. and E.Corthout (1996). The dielectric properties of biological tissues: I. literature survey. *Phys. Med. Biol.*, 41:2231–2249.

[Chauvière et al., 2006] Chauvière, C., Hesthaven, J. S., and Lurati, L. (2006). Computational modeling of uncertainty in time-domain electromagnetics. *SIAM J. Sci. Comput.*, 28(2):751–775 (electronic).

[Council,] Council, I. N. R. `http://niremf.ifac.cnr.it/tissprop/`.

[Field and Grigoriu, 2004] Field, R. V. and Grigoriu, M. (2004). On the accuracy of the polynomial chaos approximation. *Probabilistic Engineering Mechanics*, 19(1-2):65–80.

[Gaignaire et al., 2007] Gaignaire, R., Clenet, S., Sudret, B., and Moreau, O. (2007). 3D spectral stochastic finite element method in electromagnetism. *IEEE Transactions on Magnetics*, 43:1209–1212.

[Ghanem and Kruger, 1996] Ghanem, R. G. and Kruger, R. M. (1996). Numerical solution of spectral stochastic finite element systems. *Computer Methods in Applied Mechanics and Engineering*, 129(3):289–303.

[Ghanem and Spanos, 1991] Ghanem, R. G. and Spanos, P. D. (1991). *Stochastic finite elements: a spectral approach*. Springer-Verlag, New York.

[Ghiocel and Ghanem, 2002] Ghiocel, D. and Ghanem, R. G. (2002). Stochastic finite-element analysis of seismic soil-structure interaction. *Journal of Engineering Mechanics*, 128:66–77.

[Hurt et al., 2000] Hurt, W. D., Ziriax, J. M., and Mason, P. A. (2000). Variability in emf permittivity values: implications for sar calculations. *Biomedical Engineering, IEEE Transactions on*, 47(3):396–401.

[Leveque et al., 2004] Leveque, P., Dale, C., Veyret, B., and Wiart, J. (2004). Dosimetric analysis of a 900-mhz rat head exposure system. *Microwave Theory and Techniques, IEEE Transactions on*, 52(8):2076–2083.

[Newman et al., 1999] Newman, M. E. J., Barkema, G. T., and Newman, M. (1999). *Monte Carlo Methods in Statistical Physics*. Oxford University Press.

[Puig et al., 2002] Puig, B., Poirion, F., and Soize, C. (2002). Non-gaussian simulation using hermite polynomial expansion: convergences and algorithms. *Probabilistic Engineering Mechanics*, 17(3):253–264.

[Schoutens, 2000] Schoutens, W. (2000). *Stochastic processes and orthogonal polynomials*. Springer.

[Scorretti et al., 2004] Scorretti, R., Burais, N., Fabregue, O., Nicolas, A., and Nicolas, L. (2004). Computation of the induced current density into the human body due to relative lf magnetic field generated by realistic devices. *IEEE Trans. on Mag.*, 40(2):643–646.

[Stavroulakis, 2003] Stavroulakis, P. (2003). *Biological Effects of Electromagnetic Fields: mechanisms, modeling, biological effects, therapeutic effects, international standards, exposure criteria*. Springer.

[Webster et al., 1996] Webster, M. D., Tatang, M. A., and McRae, G. J. (1996). *Application of the Probabilistic Collocation Method for an Uncertainty Analysis of a Simple Ocean Model*. MIT Joint Program on the Science and Policy of Global Change.

[Wiener, 1938] Wiener, N. (1938). The Homogeneous Chaos. *Amer. J. Math.*, 60(4):897–936.

[Xiu and Hesthaven, 2005] Xiu, D. and Hesthaven, J. S. (2005). High-order collocation methods for differential equations with random inputs. *SIAM Journal on Scientific Computing*, 27(3):1118–1139.

[Xiu and Karniadakis, 2002] Xiu, D. and Karniadakis, G. E. (2002). The Wiener-Askey polynomial chaos for stochastic differential equations. *SIAM J. Sci. Comput.*, 24(2):619–644 (electronic).